Cell Reports Medicine, Volume *4*

Supplemental information

Replenishing decoy extracellular vesicles inhibits phenotype remodeling of tissue-resident cells in inflammation-driven arthritis

Mengmeng Liang, Ke Wang, Xiaoyu Wei, Xiaoshan Gong, Hao Tang, Hao Xue, Jing Wang, Pengbin Yin, Licheng Zhang, Zaisong Ma, Ce Dou, Shiwu Dong, Jianzhong Xu, Fei Luo, and Qinyu Ma

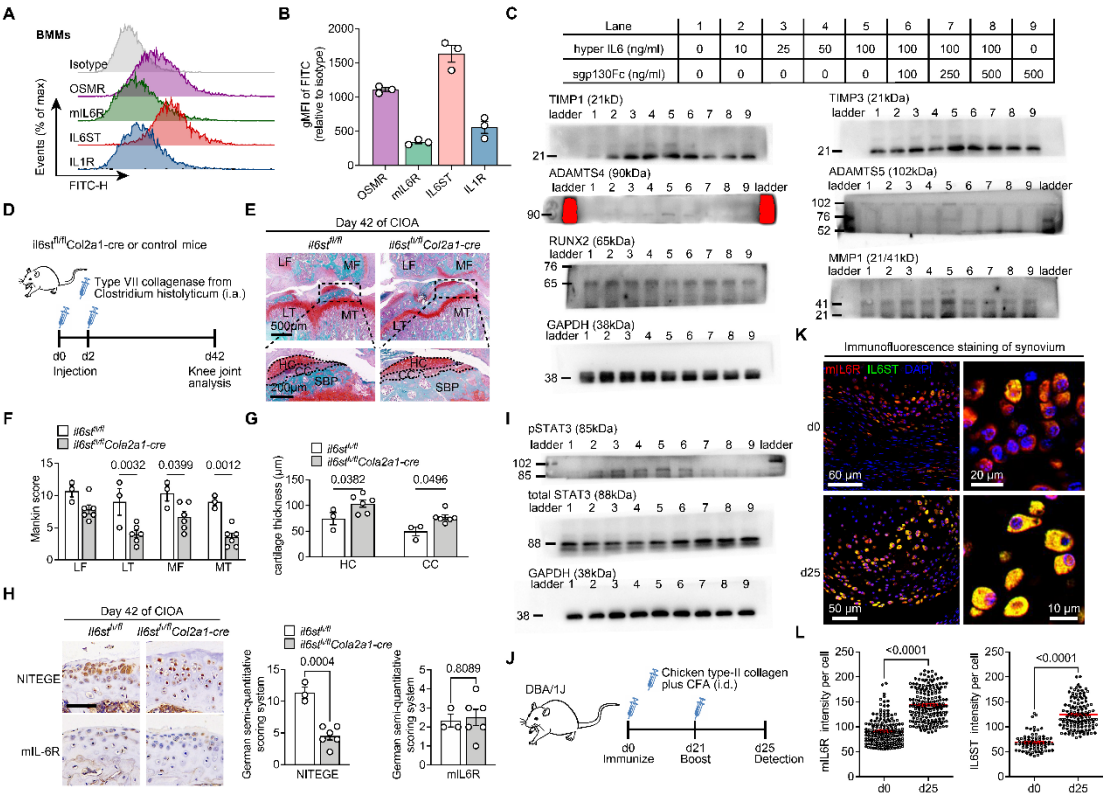

Figure S1. Response of IL6 trans-signaling by tissue-resident cells of articular joint, related to Figure 1.

(A and B) Flow cytometric histogram (A) and quantitative gMFI (B) showing the expression of respective receptor expressions including OSMR, mIL6R, IL6ST and IL1R in BMMs. *n*=3 biological replicates. gMFI, geometric mean fluorescence intensity. (C) Protein lysates were collected from cartilage explants treated with hyper IL6, sgp130Fc, or their combination at the indicated doses. Representative western blot analysis of TIMP1, TIMP3, ADAMTS4, ADAMTS5, RUNX2 and MMP1. GAPDH was used as a loading control. (D) Experimental design for assessing the effects of *il6st* depletion on the progression of OA using a CIOA mouse model. (E) Representative Safranin-O/fast green staining of the articular cartilage from *il6st*$^{fl/fl}$ mice or *il6st*$^{fl/fl}$*Col2a1-cre* mice in (D). Scale bar, 500 μm above and 200 μm below. HC and CC thickness are marked by black dashed lines. MF, medial femoral condyle. MT, medial tibial condyle. LF, lateral femoral condyle. LT, lateral tibial condyle. CC, calcified cartilage. HC, hyaline cartilage. SBP, subchondral bone plate. (F and G) Clinical Mankin score of disease progression (F) and cartilage thickness (G) in *il6st*$^{fl/fl}$*Col2a1-cre* (*n*=6) and *il6st*$^{fl/fl}$ mice (*n*=3) with CIOA induction. (H) Representative immunohistochemical staining and semiquantitative analysis of NITEGE and mIL6R in articular cartilage from *il6st*$^{fl/fl}$ mice (*n*=3) or *il6st*$^{fl/fl}$*Col2a1-cre* mice (*n*=6) at day 42 with established CIOA. Scale bars, 50 μm. (I) Protein lysates were collected from BMMs treated with hyper IL6, sgp130Fc, or their combination at the indicated doses. Representative western blot analysis of pSTAT3 and total STAT3. GAPDH was used as a loading control. (J) Experimental design for testing the ability of synovial fibroblasts in response to IL6 signaling using a CIA mouse model. (K and

L) Representative immunofluorescence staining of IL6ST and mIL6R (K) and quantification of fluorescent intensities (L). The dot plot represents the number of IL6ST or IL6ST particles from individual cells in (K). Data are presented as mean ± s.e.m. (F) and (G) Statistical significance was calculated using two-way ANOVA with Sidak's multiple comparisons test. (H) Statistical significance was calculated using Student's two-sided t-test. (L) Statistical significance was calculated using two-tailed Mann–Whitney U test.

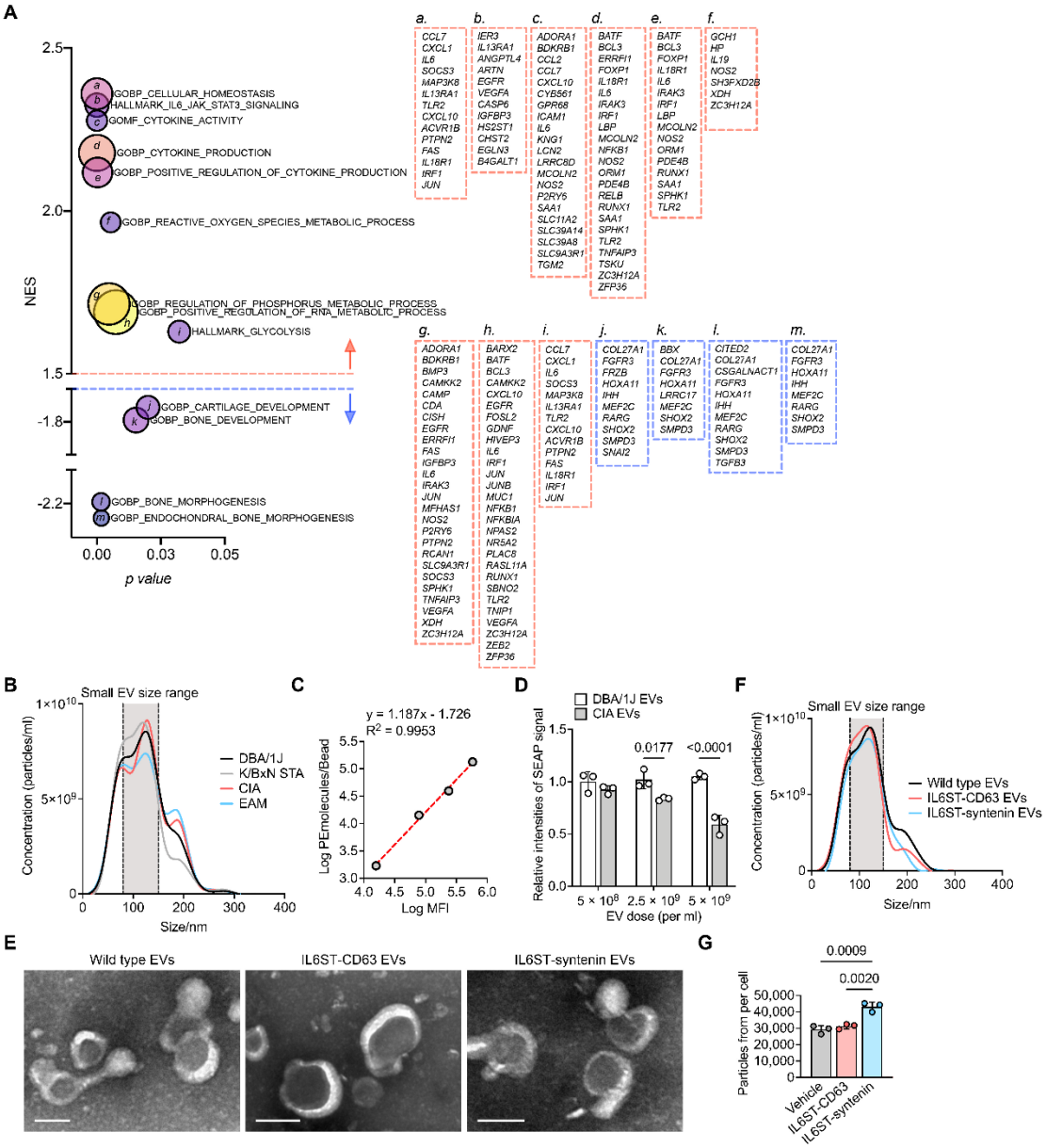

Figure S2. Identification of engineered IL6ST decoy EVs, related to Figure 2 and Figure 3.

(A) A bubble chart showing the GSEA result of a previously published RNA expression dataset of primary mouse chondrocytes treated with IL6/sIL6R. In response to IL6/sIL6R stimulation, 9 genesets related to cytokine production and cell metabolism were upregulated (as indicated by the upward red arrow) and 4 genesets related to

skeletal development and endochondral osteogenesis were downregulated (as indicated by the downward blue arrow) (left). Core enrichment genes in each geneset were listed in the dashed box (right). Red represents the upregulated genesets and blue represents the downregulated gene sets. (B) Size distribution of circulating EVs from DBA/1J, K/BxN STA, CIA and EAM mice was detected using NTA. Grey range represents the common EV size of 80 nm-150 nm. *n*=5 technical replicates. (C) Linear regression was applied to convert MFI into PE units of absolute fluorescence to delineate the receptor number examined on the EV membrane shown in (Figure 2E). (D) Relative intensities of SEAP signal in HEK-Blue IL6 Reporter cells induced by 10 ng/ml hyper IL6 and treated with EVs from CIA mice at the indicated doses. Data were normalized to HEK-Blue IL6 Reporter cells treated 5×10^8 EVs from DBA/1J mice. *n*=3 biological triplicates. (E) Representative transmission electron micrographs of EVs isolated from HEK293T cells transfected with constructs encoding IL6ST-eGFP-CD63, IL6ST-mCherry-syntenin chimeric proteins. Scale bars, 100 nm. (F) Size distribution of EVs was detected using NTA. Grey range represents the common EV size of 80 nm-150 nm. *n*=5 technical replicates. (G) The number of EVs were measured using NTA. *n*=3 biological replicates. Data are presented as mean ± s.e.m. (D) Statistical significance was calculated using two-way ANOVA with Sidak's multiple comparisons test. (G) Statistical significance was calculated using one-way ANOVA with Tukey's post hoc test for multiple comparisons.

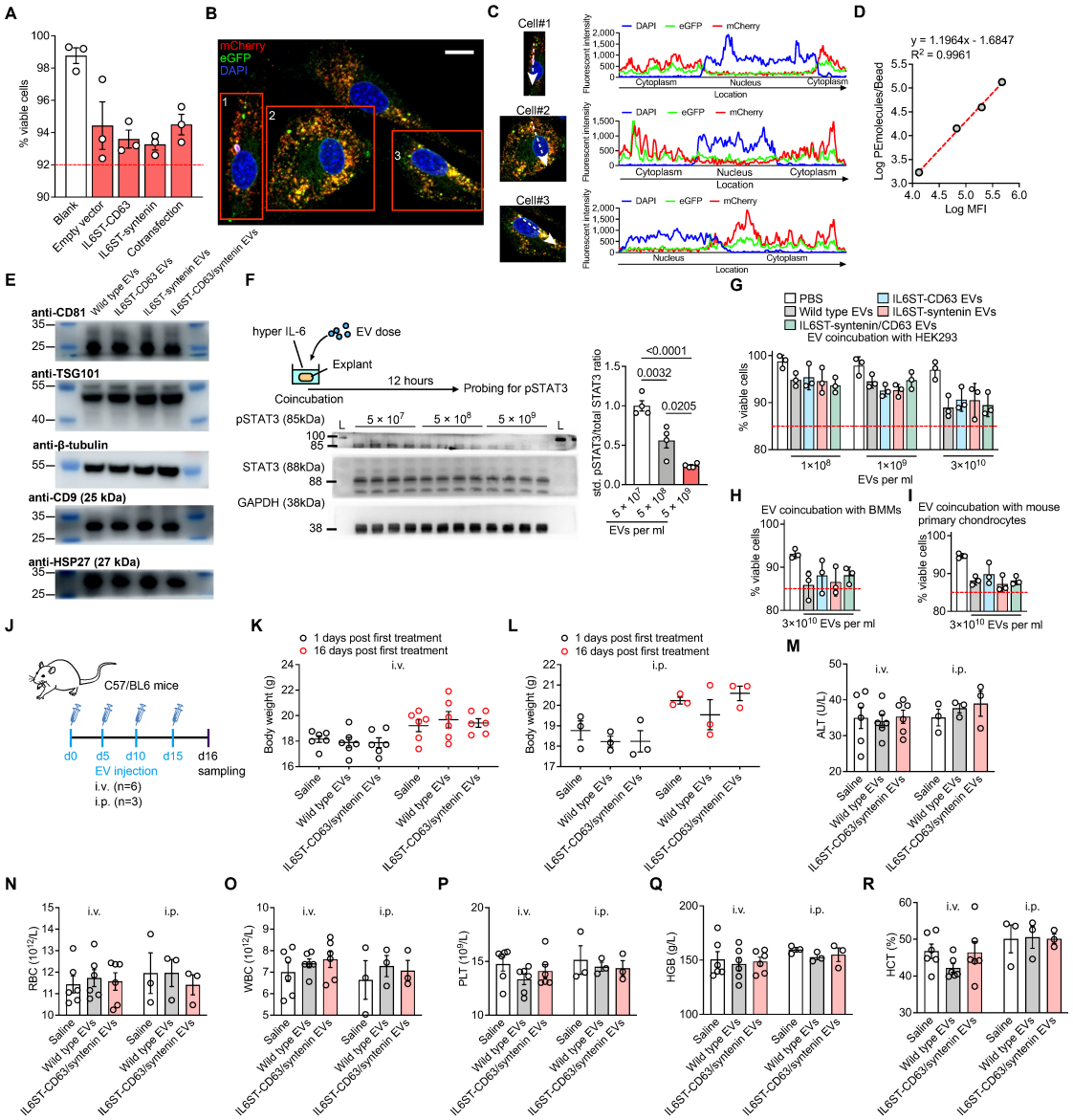

Figure S3. Characterization, function, and cytotoxicity of IL6ST decoy EVs, related to Figure 4.

(A) Cell viability of HEK293T cells transfected with respective constructs. *n*=3 biological replicates. The red dashed line indicates the tick line of 92%. (B) Representative fluorescence images showing the expression of IL6ST-eGFP-CD63 (green) and IL6ST-mCherry-syntenin (red) in HEK293T cells co-transfected with both chimeric constructs. Red boxes indicate randomly selected cells for colocalization analysis in (C). Scale bar, 10 μm. (C) Colocalization analysis of selected HEK293T cells in (B) and quantitative fluorescence intensity analysis across whole cells. White dashed arrows represent the direction of colocalization analysis. (D) Linear regression was applied to convert MFI into PE units of absolute fluorescence to delineate the receptor number examined on the EV membrane shown in (Figure 4D). (E) Protein lysates were collected from decoy EVs. Representative western blot analysis of CD81, CD9, TSG101 and HSP27. β-tubulin was used as a loading control. (F) Protein lysate was collected from mouse cartilage explants treated with 50 ng/ml hyper IL6 or IL6ST

decoy EVs at the indicated doses. Western blot analysis and quantification of pSTAT3 or total STAT3. *n*=4 biological replicates. GAPDH was used as a loading control. (G-I) Cell viability of HEK293T cells (G), BMMs (H) and primary mouse chondrocytes (I) incubated with PBS, wild type EVs, IL6ST-CD63 EVs, IL6ST-syntenin EVs or IL6ST-CD63/syntenin EVs at the indicated doses. *n*=3 biological replicates. The red dashed line indicates the tick line of 92%. (J) Experimental design for assessing the *in vivo* toxicity of decoy EV treatment. (K and L) Body weight of C57/BL6 mice administrated intravenously (K) or intraperitoneally (L) with saline, 3×10^{11} wild type EVs or 3×10^{11} IL6ST-CD63/syntenin EVs at day 1 and day 16. *n*=6 mice for intravenous injection and 3 mice for intraperitoneal injection. (M–R) Levels of ALT (M), RBC (N), WBC (O), PLT (P), HGB (Q), and HCT (R) of C57/BL6 treated intravenously or intraperitoneally with saline, 3×10^{11} wild type EVs, or 3×10^{11} IL6ST-CD63/syntenin EVs were measured at day 16. *n*=6 mice for intravenous injection and 3 mice for intraperitoneal injection. ALT, alanine aminotransferase. RBC, red blood cells. WBC, white blood cells. PLT, platelets. HGB, hemoglobin. HCT, hematocrit. Data are presented as mean ± s.e.m. (F) Statistical significance was calculated using one-way ANOVA with Tukey's post hoc test for multiple comparisons. (M)–(R) Statistical significance was calculated using two-way ANOVA with Dunnett's multiple comparisons test.

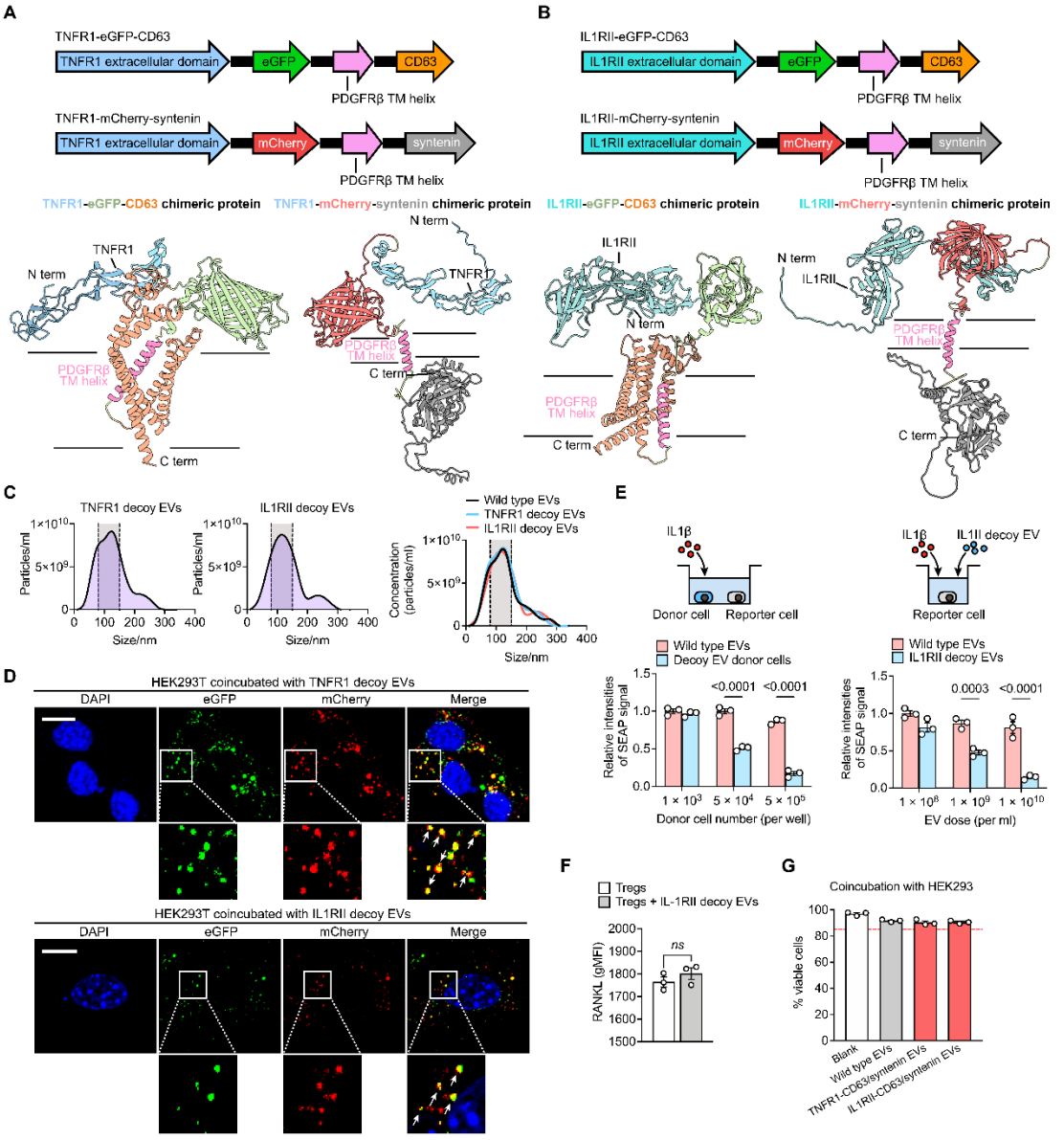

Figure S4. Construction and characterization of engineered TNFR1 and IL1RII decoy EVs, related to Figure 5.

(A) Schematic of DNA constructs expressing TNFR1-eGFP-CD63 or TNFR1-mCherry-syntenin (top). Predicted accurate model building for the intracellular, extracellular, and transmembrane domains of TNFR1-eGFP-CD63 (pLDDT=82.71), TNFR1-syntenin (pLDDT=73.35) (bottom). pLDDT greater than 70 indicates that the predicted structure has a high degree of confidence. pLDDT, predicted local-distance difference test. (B) Schematic of DNA constructs expressing of IL1RII-eGFP-CD63 or IL1RII-mCherry-syntenin chimeric protein design (top). Predicted accurate model building for the intracellular, extracellular, and transmembrane domains of IL1RII-eGFP-CD63 (pLDDT=77.07), IL1RII-syntenin (pLDDT=73.66) (bottom). pLDDT greater than 70 indicates that the predicted structure has a high degree of confidence. pLDDT, predicted local-distance difference test. (C) Size distribution of TNFR1 and IL1RII decoy EVs was detected using NTA. Grey range represents the common EV size of 80 nm-150 nm. *n*=5 technical replicates. (D) Representative fluorescence images

showing TNFR1 (top) and IL1RII (bottom) decoy EVs are internalized by HEK293 cells. Scale bars, 10 μm. (E) Schematic of reporter assay for testing the antagonistic ability of IL1RII decoy EVs or their donor cells to IL1β. Relative intensities of SEAP signal in 10 ng/ml IL1β-induced HEK-Blue IL1β Reporter cells co-cultured with EV donor cells at the indicated densities, or treated with IL1RII decoy EVs at the indicated doses. *n*=3 biological replicates. Data were normalized to cells treated with wild type HEK293T cells or wild type EVs. (F) Quantitative gMFI of RANKL expression in sorted Treg cells treated with PBS or 5 × 10^9/ml IL1RII decoy EVs. *n*=3 biological replicates. (G) Cell viability of HEK293T cells incubated with 5 × 10^9/ml wild type EVs, 5 × 10^9/ml TNFR1-CD63/syntenin EVs, or 5 × 10^9/ml IL1RII-CD63/syntenin EVs at the indicated doses. *n*=3 biological replicates. The red dashed line indicates the tick line of 92%. Data are presented as mean ± s.e.m. (E) Statistical significance was calculated using two-way ANOVA with Sidak's multiple comparisons test. (F) Statistical significance was calculated using Student's two-sided t-test.

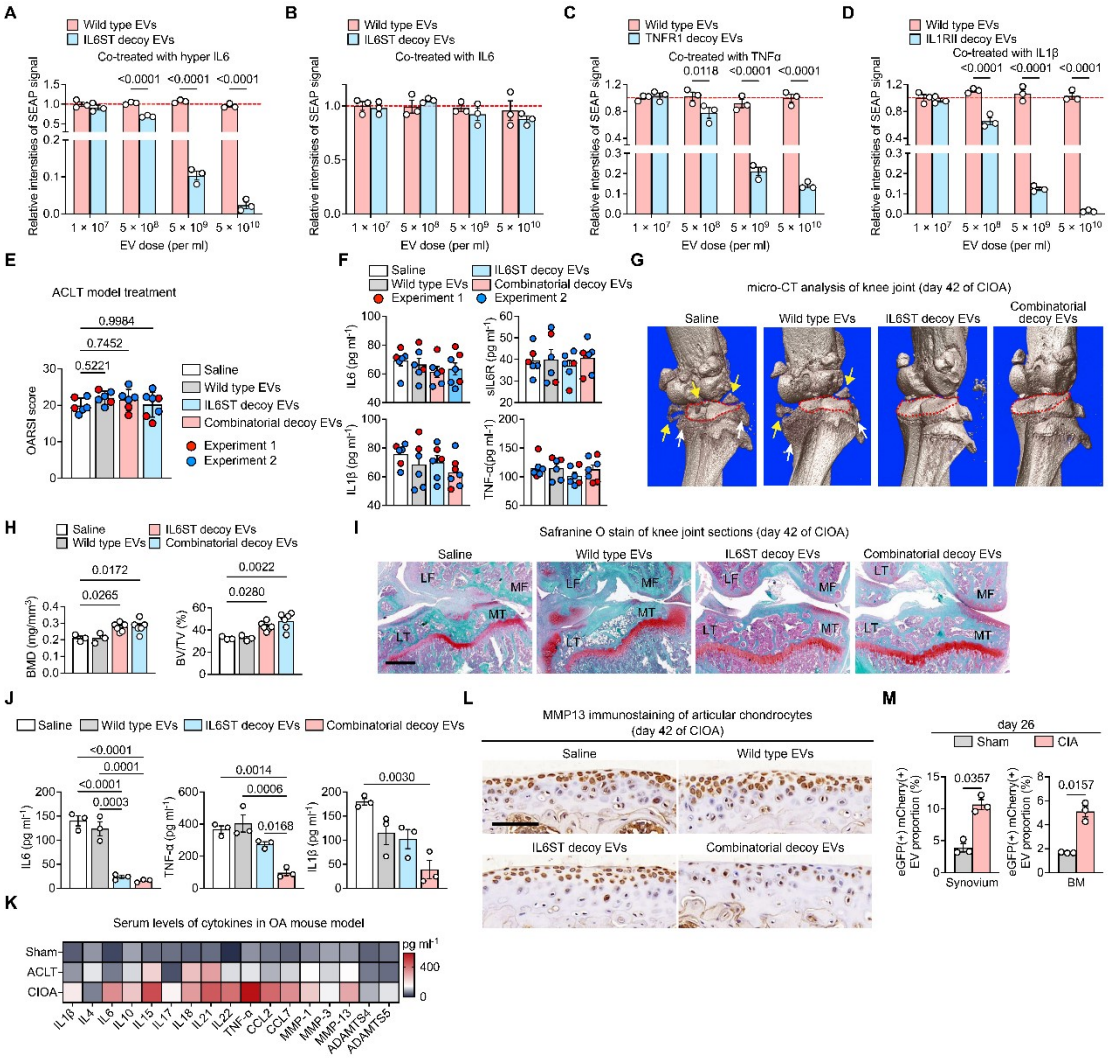

Figure S5. Decoy EVs reduced inflammation of knee joint in CIOA mice, related to Figure 6.

(A and B) Relative intensities of SEAP signal in HEK-Blue IL6 Reporter cells induced

by 10 ng/ml of either hyper IL6 (A) or IL6 (B), and treated with wild type EVs or IL6ST decoy EVs at the indicated doses. *n*=3 biological replicates. Data were normalized to cells treated with wild type EVs. (C and D) Relative intensities of SEAP signal in HEK-Blue TNFα Reporter cells induced by 5 ng/ml TNFα and treated with TNFR1 decoy EVs at the indicated doses (C), or in HEK-Blue IL1β Reporter cells induced by 10 ng/ml IL1β and treated with IL1RII decoy EVs at the indicated doses (D). *n*=3 biological replicates. Data were normalized to cells treated with wild type EVs. (E) Clinical OARSI score of disease progression in ACLT mice intraarticularly injected with saline (*n*=6), 3×10^{11} wild type EVs (*n*=6), 3×10^{11} IL6ST decoy EVs (*n*=6), or 3×10^{11} combinatorial decoy EVs (*n*=7) at the end point (day 42). (F) Serum levels of IL6, sIL6R, TNFα, or IL1β from ACLT mice treated with saline (*n*=6), 3×10^{11} wild type EVs (*n*=6), 3×10^{11} IL6ST decoy EVs (*n*=6), or 3×10^{11} combinatorial EVs (*n*=7). Cytokines were measured using Luminex assay. (G) Representative micro-CT images of articular joint of CIOA mice treated with saline, 3×10^{11} wild type EVs, 3×10^{11} IL6ST decoy EVs, or 3×10^{11} combinatorial decoy EVs. White arrows denote newly formed osteophytes. Yellow arrows denote calcified tissues. Red dotted area indicates the surface of tibial plateau. (H) Quantification of bone mineral density (BMD) and trabecular bone volume fraction (BV/TV) in the subchondral bone. (I) Representative Safranin-O/fast green staining of CIOA mice treated with saline, 3×10^{11} wild type EVs, 3×10^{11} IL6ST decoy EVs, or 3×10^{11} combinatorial decoy EVs. Scale bar, 500 μm. MF, medial femoral condyle; MT, medial tibial condyle; LF, lateral femoral condyle, LT, lateral tibial condyle. (J) Serum levels of IL6, TNFα, or IL1β from CIOA mice treated with saline, 3×10^{11} wild type EVs, 3×10^{11} IL6ST decoy EVs, or 3×10^{11} combinatorial EVs. *n*=3 biological replicates. Cytokines were measured using Luminex assay. (K) Heatmap showing the expression of interleukins, chemokines, and matrix enzymes in serum from sham, ACLT and CIA mice. Each cell of heatmap represents the average expression value of cytokines from three technical replicates. Cytokines were measured using Luminex assay. (L) Representative immunostaining of MMP13 in articular cartilage from CIOA mice treated with saline, 3×10^{11} wild type EVs, 3×10^{11} IL6ST decoy EVs, or 3×10^{11} combinatorial EVs. Scale bars, 100 μm. (M) Proportion of $eGFP^{+}/mCherry^{+}$ EV population in synovial tissue and bone marrow from sham mice (*n*=3) and CIA mice (*n*=3) were measured using flow cytometry. Data are presented as mean ± s.e.m. (A)–(D) Statistical significance was calculated using two-way ANOVA with Sidak's multiple comparisons test. (E), (F), (H) and (J) Statistical significance was calculated using one-way ANOVA with Tukey's post hoc test for multiple comparisons. (M) Statistical significance was calculated using Student's two-sided t-test.

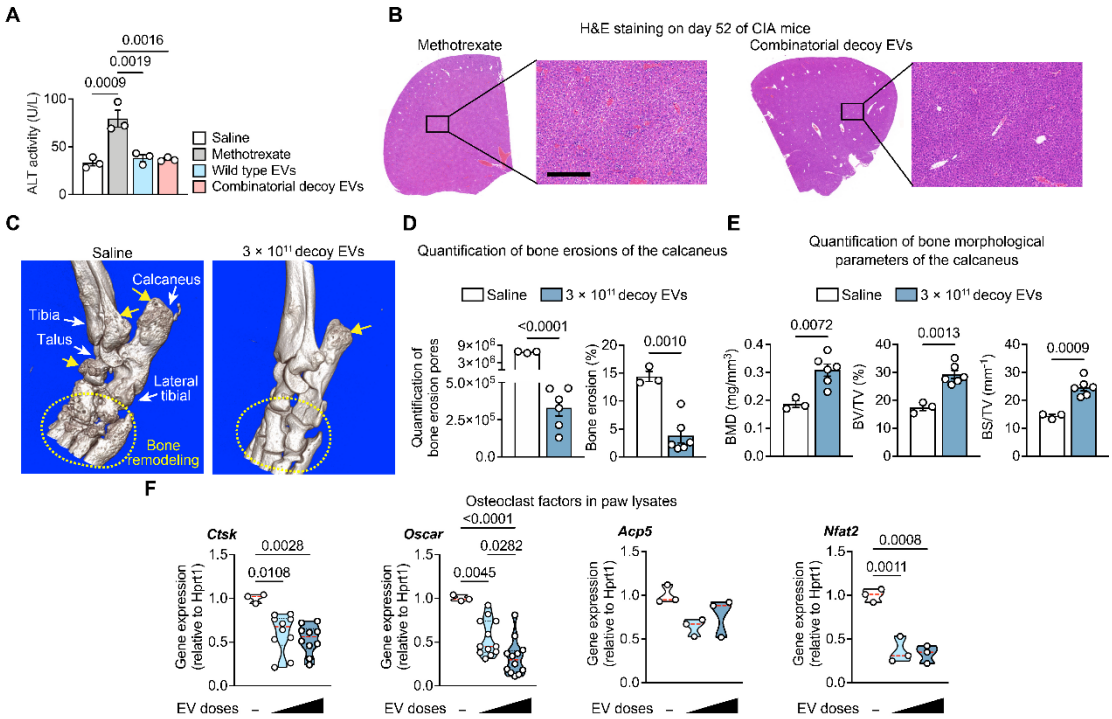

Figure S6. Decoy EVs safely and efficiently relieves systemic inflammatory arthritis, related to Figure 6.

(A) Quantification of ALT activity of CIA mice at the end point (day 52). *n*=3 biological replicates. (B) Representative H&E staining of liver samples from CIA mice at the end point (day 52). Scale bar, 300 μm. (C) Representative micro-CT images of the ankle joints of CIA mice at day 52. The significant bone remodeling in CIA mice treated with saline, indicated by yellow arrows and dotted area, was significantly reduced in CIA mice treated with 3×10^{11} decoy EVs. (D) Bone erosions were quantified in the area of the calcaneus of CIA mice treated with saline (*n*=3) or 3×10^{11} decoy EVs (*n*=6). (E) Quantification of bone mineral density (BMD), trabecular bone volume fraction (BV/TV) and bone surface density (BS/TV) of the calcaneus. (F) Relative gene expression of osteoclast factors including *Ctsk*, *Oscar*, *Acp5* and *Nfat2* in paw lysates from CIA mice were measured using RT-qPCR. *n*=3–10 biological replicates. Data are presented as mean ± s.e.m. (A) and (F) Statistical significance was calculated using one-way ANOVA with Tukey's post hoc test for multiple comparisons. (D) and (E) Statistical significance was calculated using Student's two-sided t-test.

Table S1. Protein sequence of the chimeric proteins composed of decoy receptors, fluorescent proteins, and EV-sorting proteins, related to Figure 3 and Figure 4.

Chimeric protein	Protein sequence
IL6ST-eGFP-CD63 (Mw: 124 kDa)	MSAPRIWLAQALLFFLTTESIGQLLEPCGYIYPEFPVVQRGSNFTAICVLK EACLQHYYVNASYIVWKTNHAAVPREQVTVINRTTSSVTFTDVVLPSV QLTCNILSFGQIEQNVYGVTMLSGFPPDKPTNLTCIVNEGKNMLCQWDP GRETYLETNYTLKSEWATEKFPDCQSKHGTSCMVSYMPTYYVNIEVW VEAENALGKVSSESINFDPVDKVKPTPPYNLSVTNSEELSSILKLSWVSS GLGGLLDLKSDIQYRTKDASTWIQVPLEDTMSPRTSFTVQDLKPFTEYV FRIRSIKDSGKGYWSDWSEEASGTTYEDRPSRPPSFWYKTNPSHGQEYR SVRLIWKALPLSEANGKILDYEVILTQSKSVSQTYTVTGTELTVNLTNDR YVASLAARNKVGKSAAAVLTIPSPHVTAAYSVVNLKAFPKDNLLWVEW TPPPKPVSKYILEWCVLSENAPCVEDWQQEDATVNRTHLRGRLLESKC YQITVTPVFATGPGGSESLKAYLKQAAPARGPTVRTKKVGKNEAVLAW DQIPVDDQNGFIRNYSISYRTSVGKEMVVHVDSSHTEYTLSSLSSDTLY MVRMAAYTDEGGKDGPEFTFTTPKFAGGGGSMVSKGEELFTGVVPILV ELDGDVNGHKFSVSGEGEGDATYGKLTLKFICTTGKLPVPWPTLVTTLT YGVQCFSRYPDHMKQHDFFKSAMPEGYVQERTIFFKDDGNYKTRAEV KFEGDTLVNRIELKGIDFKEDGNILGHKLEYNYNSHNVYIMADKQKNGI KVNFKIRHNIEDGSVQLADHYQQNTPIGDGPVLLPDNHYLSTQSALSKD PNEKRDHMVLLEFVTAAGITLGMDELYKGGGGSVVISAILALVVLTIISLI ILIGGGGSAVEGGMKCVKFLLYVLLLAFCACAVGLIAVGVGAQLVLSQT IIQGATPGSLLPVVIIAVGVFLFLVAFVGCCGACKENYCLMITFAIFLSLIM LVEVAAAIAGYVFRDKVMSEFNNNFRQQMENYPKNNHTASILDRMQA DFKCCGAANYTDWEKIPSMSKNRVPDSCCINVTVGCGINFNEKAIHKE GCVEKIGGWLRKNVLVVAAAALGIAFVEVLGIVFACCLVKSIRSGYEVM
IL6ST-mCherry-syntenin (Mw: 130 kDa)	MSAPRIWLAQALLFFLTTESIGQLLEPCGYIYPEFPVVQRGSNFTAICVLK EACLQHYYVNASYIVWKTNHAAVPREQVTVINRTTSSVTFTDVVLPSV QLTCNILSFGQIEQNVYGVTMLSGFPPDKPTNLTCIVNEGKNMLCQWDP GRETYLETNYTLKSEWATEKFPDCQSKHGTSCMVSYMPTYYVNIEVW VEAENALGKVSSESINFDPVDKVKPTPPYNLSVTNSEELSSILKLSWVSS GLGGLLDLKSDIQYRTKDASTWIQVPLEDTMSPRTSFTVQDLKPFTEYV FRIRSIKDSGKGYWSDWSEEASGTTYEDRPSRPPSFWYKTNPSHGQEYR SVRLIWKALPLSEANGKILDYEVILTQSKSVSQTYTVTGTELTVNLTNDR YVASLAARNKVGKSAAAVLTIPSPHVTAAYSVVNLKAFPKDNLLWVEW TPPPKPVSKYILEWCVLSENAPCVEDWQQEDATVNRTHLRGRLLESKC YQITVTPVFATGPGGSESLKAYLKQAAPARGPTVRTKKVGKNEAVLAW DQIPVDDQNGFIRNYSISYRTSVGKEMVVHVDSSHTEYTLSSLSSDTLY MVRMAAYTDEGGKDGPEFTFTTPKFAGGGGSMVSKGEEDNMAIIKEF MRFKVHMEGSVNGHEFEIEGEGEGRPYEGTQTAKLKVTKGGPLPFAWD ILSPQFMYGSKAYVKHPADIPDYLKLSFPEGFKWERVMNFEDGGVVTV TQDSSLQDGEFIYKVKLRGTNFPSDGPVMQKKTMGWEASSERMYPED

	GALKGEIKQRLKLKDGGHYDAEVKTTYKAKKPVQLPGAYNVNIKLDIT SHNEDYTIVEQYERAEGRHSTGGMDELYKGGGGSVVISAILALVVLTIIS LIILIGGGGSMSLYPSLEDLKVDKVIQAQTAFSANPANPAILSEASAPIPHD GNLYPRLYPELSQYMGLSLNEEEIRANVAVVSGAPLQGQLVARPSSINY MVAPVTGNDVGIRRAEIKQGIREVILCKDQDGKIGLRLKSIDNGIFVQLV QANSPASLVGLRFGDQVLQINGENCAGWSSDKAHKVLKQAFGEKITMT IRDRPFERTITMHKDSTGHVGFIFKNGKITSIVKDSSAARNGLLTEHNICE INGQNVIGLKDSQIADILSTSGTVVTITIMPAFIFEHIIKRMAPSIMKSLMD HTIPEV
TNFR1-eGFP-CD63 (Mw: 77 kDa)	MGLPTVPGLLLSLVLLALLMGIHPSGVTGLVPSLGDREKRDSLCPQGKY VHSKNNSICCTKCHKGTYLVSDCPSPGRDTVCRECEKGTFTASQNYLRQ CLSCKTCRKEMSQVEISPCQADKDTVCGCKENQFQRYLSETHFQCVDC SPCFNGTVTIPCKETQNTVCNCHAGFFLRESECVPCSHCKKNEECMKLC LPGGGGSMVSKGEELFTGVVPILVELDGDVNGHKFSVSGEGEGDATYG KLTLKFICTTGKLPVPWPTLVTTLTYGVQCFSRYPDHMKQHDFFKSAMP EGYVQERTIFFKDDGNYKTRAEVKFEGDTLVNRIELKGIDFKEDGNILG HKLEYNYNSHNVYIMADKQKNGIKVNFKIRHNIEDGSVQLADHYQQN TPIGDGPVLLPDNHYLSTQSALSKDPNEKRDHMVLLEFVTAAGITLGMD ELYKGGGGSVVISAILALVVLTIISLIILIGGGGSAVEGGMKCVKFLLYVL LLAFCACAVGLIAVGVGAQLVLSQTIIQGATPGSLLPVVIIAVGVFLFLVA FVGCCGACKENYCLMITFAIFLSLIMLVEVAAAIAGYVFRDKVMSEFNN NFRQQMENYPKNNHTASILDRMQADFKCCGAANYTDWEKIPSMSKNR VPDSCCINVTVGCGINFNEKAIHKEGCVEKIGGWLRKNVLVVAAAALGI AFVEVLGIVFACCLVKSIRSGYEVM
TNFR1-mCherry-syntenin (Mw: 83 kDa)	MGLPTVPGLLLSLVLLALLMGIHPSGVTGLVPSLGDREKRDSLCPQGKY VHSKNNSICCTKCHKGTYLVSDCPSPGRDTVCRECEKGTFTASQNYLRQ CLSCKTCRKEMSQVEISPCQADKDTVCGCKENQFQRYLSETHFQCVDC SPCFNGTVTIPCKETQNTVCNCHAGFFLRESECVPCSHCKKNEECMKLC LPGGGGSMVSKGEEDNMAIIKEFMRFKVHMEGSVNGHEFEIEGEGEGR PYEGTQTAKLKVTKGGPLPFAWDILSPQFMYGSKAYVKHPADIPDYLKL SFPEGFKWERVMNFEDGGVVTVTQDSSLQDGEFIYKVKLRGTNFPSDG PVMQKKTMGWEASSERMYPEDGALKGEIKQRLKLKDGGHYDAEVKT TYKAKKPVQLPGAYNVNIKLDITSHNEDYTIVEQYERAEGRHSTGGMD ELYKGGGGSVVISAILALVVLTIISLIILIGGGGSMSLYPSLEDLKVDKVIQ AQTAFSANPANPAILSEASAPIPHDGNLYPRLYPELSQYMGLSLNEEEIRA NVAVVSGAPLQGQLVARPSSINYMVAPVTGNDVGIRRAEIKQGIREVILC KDQDGKIGLRLKSIDNGIFVQLVQANSPASLVGLRFGDQVLQINGENCA GWSSDKAHKVLKQAFGEKITMTIRDRPFERTITMHKDSTGHVGFIFKNG KITSIVKDSSAARNGLLTEHNICEINGQNVIGLKDSQIADILSTSGTVVTIT IMPAFIFEHIIKRMAPSIMKSLMDHTIPEV
IL1RII-eGFP-CD63 (Mw: 95 kDa)	MFILLVLVTGVSAFTTPTVVHTGKVSESPITSEKPTVHGDNCQFRGREFK SELRLEGEPVVLRCPLAPHSDISSSSHSFLTWSKLDSSQLIPRDEPRMWV KGNILWILPAVQQDSGTYICTFRNASHCEQMSVELKVFKNTEASLPHVS YLQISALSTTGLLVCPDLKEFISSNADGKIQWYKGAILLDKGNKEFLSAG

	DPTRLLISNTSMDDAGYYRCVMTFTYNGQEYNITRNIELRVKGTTTEPIP VIISPLETIPASLGSRLIVPCKVFLGTGTSSNTIVWWLANSTFISAAYPRGR VTEGLHHQYSENDENYVEVSLIFDPVTREDLHTDFKCVASNPRSSQSLH TTVKEVSSGGGGSMVSKGEELFTGVVPILVELDGDVNGHKFSVSGEGE GDATYGKLTLKFICTTGKLPVPWPTLVTTLTYGVQCFSRYPDHMKQHDF FKSAMPEGYVQERTIFFKDDGNYKTRAEVKFEGDTLVNRIELKGIDFKE DGNILGHKLEYNYNSHNVYIMADKQKNGIKVNFKIRHNIEDGSVQLAD HYQQNTPIGDGPVLLPDNHYLSTQSALSKDPNEKRDHMVLLEFVTAAG ITLGMDELYKGGGGSVVISAILALVVLTIISLIILIGGGGSAVEGGMKCVK FLLYVLLLAFCACAVGLIAVGVGAQLVLSQTIIQGATPGSLLPVVIIAVGV FLFLVAFVGCCGACKENYCLMITFAIFLSLIMLVEVAAAIAGYVFRDKV MSEFNNNFRQQMENYPKNNHTASILDRMQADFKCCGAANYTDWEKIP SMSKNRVPDSCCINVTVGCGINFNEKAIHKEGCVEKIGGWLRKNVLVV AAAALGIAFVEVLGIVFACCLVKSIRSGYEVM
IL1RII- mCherry- syntenin (Mw: 102 kDa)	MFILLVLVTGVSAFTTPTVVHTGKVSESPITSEKPTVHGDNCQFRGREFK SELRLEGEPVVLRCPLAPHSDISSSSHSFLTWSKLDSSQLIPRDEPRMWV KGNILWILPAVQQDSGTYICTFRNASHCEQMSVELKVFKNTEASLPHVS YLQISALSTTGLLVCPDLKEFISSNADGKIQWYKGAILLDKGNKEFLSAG DPTRLLISNTSMDDAGYYRCVMTFTYNGQEYNITRNIELRVKGTTTEPIP VIISPLETIPASLGSRLIVPCKVFLGTGTSSNTIVWWLANSTFISAAYPRGR VTEGLHHQYSENDENYVEVSLIFDPVTREDLHTDFKCVASNPRSSQSLH TTVKEVSSGGGGSMVSKGEEDNMAIIKEFMRFKVHMEGSVNGHEFEIE GEGEGRPYEGTQTAKLKVTKGGPLPFAWDILSPQFMYGSKAYVKHPADI PDYLKLSFPEGFKWERVMNFEDGGVVTVTQDSSLQDGEFIYKVKLRGT NFPSDGPVMQKKTMGWEASSERMYPEDGALKGEIKQRLKLKDGGHY DAEVKTTYKAKKPVQLPGAYNVNIKLDITSHNEDYTIVEQYERAEGRH STGGMDELYKGGGGSVVISAILALVVLTIISLIILIGGGGSMSLYPSLEDLK VDKVIQAQTAFSANPANPAILSEASAPIPHDGNLYPRLYPELSQYMGLSL NEEEIRANVAVVSGAPLQGQLVARPSSINYMVAPVTGNDVGIRRAEIKQ GIREVILCKDQDGKIGLRLKSIDNGIFVQLVQANSPASLVGLRFGDQVLQ INGENCAGWSSDKAHKVLKQAFGEKITMTIRDRPFERTITMHKDSTGH VGFIFKNGKITSIVKDSSAARNGLLTEHNICEINGQNVIGLKDSQIADILS TSGTVVTITIMPAFIFEHIIKRMAPSIMKSLMDHTIPEV

Table S2. Protein sequence of the chimeric proteins with fluorescent proteins removed, related to Figure 6.

Chimeric protein	Protein sequence
IL6ST-CD63 (Mw: 96 kDa)	MSAPRIWLAQALLFFLTTESIGQLLEPCGYIYPEFPVVQRGSNFTAICVLKEA CLQHYYVNASYIVWKTNHAAVPREQVTVINRTTSSVTFTDVVLPSVQLTCN ILSFGQIEQNVYGVTMLSGFPPDKPTNLTCIVNEGKNMLCQWDPGRETYLE TNYTLKSEWATEKFPDCQSKHGTSCMVSYMPTYYVNIEVWVEAENALGK VSSESINFDPVDKVKPTPPYNLSVTNSEELSSILKLSWVSSGLGGLLDLKSDI QYRTKDASTWIQVPLEDTMSPRTSFTVQDLKPFTEYVFRIRSIKDSGKGYW SDWSEEASGTTYEDRPSRPPSFWYKTNPSHGQEYRSVRLIWKALPLSEANG KILDYEVILTQSKSVSQTYTVTGTELTVNLTNDRYVASLAARNKVGKSAAA VLTIPSPHVTAAYSVVNLKAFPKDNLLWVEWTPPPKPVSKYILEWCVLSEN APCVEDWQQEDATVNRTHLRGRLLESKCYQITVTPVFATGPGGSESLKAYL KQAAPARGPTVRTKKVGKNEAVLAWDQIPVDDQNGFIRNYSISYRTSVGK EMVVHVDSSHTEYTLSSLSSDTLYMVRMAAYTDEGGKDGPEFTFTTPKFA GGGGSVVISAILALVVLTIISLIILIGGGGSAVEGGMKCVKFLLYVLLLAFCA CAVGLIAVGVGAQLVLSQTIIQGATPGSLLPVVIIAVGVFLFLVAFVGCCGAC KENYCLMITFAIFLSLIMLVEVAAAIAGYVFRDKVMSEFNNNFRQQMENYP KNNHTASILDRMQADFKCCGAANYTDWEKIPSMSKNRVPDSCCINVTVGC GINFNEKAIHKEGCVEKIGGWLRKNVLVVAAAALGIAFVEVLGIVFACCLV KSIRSGYEVM
IL6ST-syntenin (Mw: 103 kDa)	MSAPRIWLAQALLFFLTTESIGQLLEPCGYIYPEFPVVQRGSNFTAICVLKEA CLQHYYVNASYIVWKTNHAAVPREQVTVINRTTSSVTFTDVVLPSVQLTCN ILSFGQIEQNVYGVTMLSGFPPDKPTNLTCIVNEGKNMLCQWDPGRETYLE TNYTLKSEWATEKFPDCQSKHGTSCMVSYMPTYYVNIEVWVEAENALGK VSSESINFDPVDKVKPTPPYNLSVTNSEELSSILKLSWVSSGLGGLLDLKSDI QYRTKDASTWIQVPLEDTMSPRTSFTVQDLKPFTEYVFRIRSIKDSGKGYW SDWSEEASGTTYEDRPSRPPSFWYKTNPSHGQEYRSVRLIWKALPLSEANG KILDYEVILTQSKSVSQTYTVTGTELTVNLTNDRYVASLAARNKVGKSAAA VLTIPSPHVTAAYSVVNLKAFPKDNLLWVEWTPPPKPVSKYILEWCVLSEN APCVEDWQQEDATVNRTHLRGRLLESKCYQITVTPVFATGPGGSESLKAYL KQAAPARGPTVRTKKVGKNEAVLAWDQIPVDDQNGFIRNYSISYRTSVGK EMVVHVDSSHTEYTLSSLSSDTLYMVRMAAYTDEGGKDGPEFTFTTPKFA GGGGSVVISAILALVVLTIISLIILIGGGGSMSLYPSLEDLKVDKVIQAQTAFS ANPANPAILSEASAPIPHDGNLYPRLYPELSQYMGLSLNEEEIRANVAVVSG APLQGQLVARPSSINYMVAPVTGNDVGIRRAEIKQGIREVILCKDQDGKIGL RLKSIDNGIFVQLVQANSPASLVGLRFGDQVLQINGENCAGWSSDKAHKVL KQAFGEKITMTIRDRPFERTITMHKDSTGHVGFIFKNGKITSIVKDSSAARN GLLTEHNICEINGQNVIGLKDSQIADILSTSGTVVTITIMPAFIFEHIIKRMAPS IMKSLMDHTIPEV
TNFR1-CD63	MGLPTVPGLLLSLVLLALLMGIHPSGVTGLVPSLGDREKRDSLCPQGKYVH SKNNSICCTKCHKGTYLVSDCPSPGRDTVCRECEKGTFTASQNYLRQCLSC

(Mw: 50 kDa)	KTCRKEMSQVEISPCQADKDTVCGCKENQFQRYLSETHFQCVDCSPCFNG TVTIPCKETQNTVCNCHAGFFLRESECVPCSHCKKNEECMKLCLPGGGGS VVISAILALVVLTIISLIILIGGGGSAVEGGMKCVKFLLYVLLLAFCACAVGLI AVGVGAQLVLSQTIIQGATPGSLLPVVIIAVGVFLFLVAFVGCCGACKENYC LMITFAIFLSLIMLVEVAAAIAGYVFRDKVMSEFNNNFRQQMENYPKNNHT ASILDRMQADFKCCGAANYTDWEKIPSMSKNRVPDSCCINVTVGCGINFN EKAIHKEGCVEKIGGWLRKNVLVVAAAALGIAFVEVLGIVFACCLVKSIRS GYEVM
TNFR1-syntenin (Mw: 56 kDa)	MGLPTVPGLLLSLVLLALLMGIHPSGVTGLVPSLGDREKRDSLCPQGKYVH SKNNSICCTKCHKGTYLVSDCPSPGRDTVCRECEKGTFTASQNYLRQCLSC KTCRKEMSQVEISPCQADKDTVCGCKENQFQRYLSETHFQCVDCSPCFNG TVTIPCKETQNTVCNCHAGFFLRESECVPCSHCKKNEECMKLCLPGGGGS VVISAILALVVLTIISLIILIGGGGSMSLYPSLEDLKVDKVIQAQTAFSANPAN PAILSEASAPIPHDGNLYPRLYPELSQYMGLSLNEEEIRANVAVVSGAPLQG QLVARPSSINYMVAPVTGNDVGIRRAEIKQGIREVILCKDQDGKIGLRLKSI DNGIFVQLVQANSPASLVGLRFGDQVLQINGENCAGWSSDKAHKVLKQAF GEKITMTIRDRPFERTITMHKDSTGHVGFIFKNGKITSIVKDSSAARNGLLTE HNICEINGQNVIGLKDSQIADILSTSGTVVTITIMPAFIFEHIIKRMAPSIMKSL MDHTIPEV
IL1RII-CD63 (Mw: 68 kDa)	MFILLVLVTGVSAFTTPTVVHTGKVSESPITSEKPTVHGDNCQFRGREFKSE LRLEGEPVVLRCPLAPHSDISSSSHSFLTWSKLDSSQLIPRDEPRMWVKGNI LWILPAVQQDSGTYICTFRNASHCEQMSVELKVFKNTEASLPHVSYLQISAL STTGLLVCPDLKEFISSNADGKIQWYKGAILLDKGNKEFLSAGDPTRLLISN TSMDDAGYYRCVMTFTYNGQEYNITRNIELRVKGTTTEPIPVIISPLETIPAS LGSRLIVPCKVFLGTGTSSNTIVWWLANSTFISAAYPRGRVTEGLHHQYSE NDENYVEVSLIFDPVTREDLHTDFKCVASNPRSSQSLHTTVKEVSSGGGGS VVISAILALVVLTIISLIILIGGGGSAVEGGMKCVKFLLYVLLLAFCACAVGLI AVGVGAQLVLSQTIIQGATPGSLLPVVIIAVGVFLFLVAFVGCCGACKENYC LMITFAIFLSLIMLVEVAAAIAGYVFRDKVMSEFNNNFRQQMENYPKNNHT ASILDRMQADFKCCGAANYTDWEKIPSMSKNRVPDSCCINVTVGCGINFN EKAIHKEGCVEKIGGWLRKNVLVVAAAALGIAFVEVLGIVFACCLVKSIRS GYEVM
IL1RII-syntenin (Mw: 74 kDa)	MFILLVLVTGVSAFTTPTVVHTGKVSESPITSEKPTVHGDNCQFRGREFKSE LRLEGEPVVLRCPLAPHSDISSSSHSFLTWSKLDSSQLIPRDEPRMWVKGNI LWILPAVQQDSGTYICTFRNASHCEQMSVELKVFKNTEASLPHVSYLQISAL STTGLLVCPDLKEFISSNADGKIQWYKGAILLDKGNKEFLSAGDPTRLLISN TSMDDAGYYRCVMTFTYNGQEYNITRNIELRVKGTTTEPIPVIISPLETIPAS LGSRLIVPCKVFLGTGTSSNTIVWWLANSTFISAAYPRGRVTEGLHHQYSE NDENYVEVSLIFDPVTREDLHTDFKCVASNPRSSQSLHTTVKEVSSGGGGS VVISAILALVVLTIISLIILIGGGGSMSLYPSLEDLKVDKVIQAQTAFSANPAN PAILSEASAPIPHDGNLYPRLYPELSQYMGLSLNEEEIRANVAVVSGAPLQG QLVARPSSINYMVAPVTGNDVGIRRAEIKQGIREVILCKDQDGKIGLRLKSI DNGIFVQLVQANSPASLVGLRFGDQVLQINGENCAGWSSDKAHKVLKQAF GEKITMTIRDRPFERTITMHKDSTGHVGFIFKNGKITSIVKDSSAARNGLLTE

	HNICEINGQNVIGLKDSQIADILSTSGTVVTITIMPAFIFEHIIKRMAPSIMKSL MDHTIPEV

Table S3. Primer sequences for qPCR, related to Figure 6.

Genes	Forward	Reverse	Tm (°C)
Ctsk	5'-GAAGAAGACTCACCAGAAGCAG-3'	5'-TCCAGGTTATGGGCAGAGATT-3'	61
Oscar	5'-CCTAGCCTCATACCCCCAG-3'	5'-CGTTGATCCCAGGAGTCACAA-3'	60
Acp5	5'-CACTCCCACCCTGAGATTTGT-3'	5'-CATCGTCTGCACGGTTCTG-3'	61
Nfat2	5'-GACCCGGAGTTCGACTTCG-3'	5'-TGACACTAGGGGACACATAACTG-3'	62
Hprt1	5'-TCAGTCAACGGGGGACATAAA-3'	5'-GGGGCTGTACTGCTTAACCAG-3'	62